Design, Synthesis, and Biological Evaluation of CXCR4 ligands

Christine E. Mona,[a,d] Élie Besserer-Offroy,[a,d] Jérôme Cabana,[a,d] Richard Leduc,[a,d] Pierre Lavigne,[b,d] Nikolaus Heveker,[c] Éric Marsault,[a,d]* Emanuel Escher,[a,d]*

[a]*Department of Pharmacology-Physiology, Université de Sherbrooke, Sherbrooke, QC, Canada;* [b]*Department of Biochemistry, Université de Sherbrooke, Sherbrooke, QC, Canada;* [c]*Department of Biochemistry and Molecular Medicine, Centre de Recherche Hôpital Sainte-Justine, Université de Montréal, Montreal, QC, Canada;* [d]*Institut de Pharmacologie de Sherbrooke, Université de Sherbrooke, Sherbrooke, QC, Canada.*

* *Corresponding Authors*

Emanuel Escher

3001, 12e avenue Nord, J1H 5N4 Sherbrooke, QC, Canada

Emanuel.Escher@usherbrooke.ca

Phone: +1 819.821.8000 ext: 75341 Fax: +1 819.564.5400

Eric Marsault

3001, 12e avenue Nord, J1H 5N4 Sherbrooke, QC, Canada

Phone: +1 819.821.8000 ext: 72433 Fax: +1 819.564.5400

Eric.Marsault@usherbrooke.ca

Keywords: chemokine receptor, chemotaxis, CXCR4, inverse agonist SAR, structure

ABSTRACT:

Combination of the CXCR4 inverse agonist T140 with N-terminal CXCL12 oligopeptides has produced the first nanomolar synthetic CXCR4 agonists. In those agonists, the inverse agonistic portion provides affinity whereas the N-terminal CXCL12 sequence induces receptor activation. Several CXCR4 crystal structures exist with either CVX15, an inverse agonist closely related to T140 and IT1t, a small molecule; we therefore attempted to produce another CXCL12 oligopeptide combination with IT1t. For this purpose, a primary amino group was introduced by total synthesis into one of the methyl groups of IT1t, serving as anchoring point for the oligopeptide graft. The introduction of the oligopeptides on this analog however yielded antagonists, one compound displaying high affinity. On the other hand, the aminosubstituted analogue itself proved to be an inverse agonist with a binding affinity of 2.6 nM compared to 11.5 nM for IT1t. This IT1t-like analog is hitherto one of the most potent non peptidic CXCR4 inverse agonist reported.

GRAPHICAL ABSTRACT:

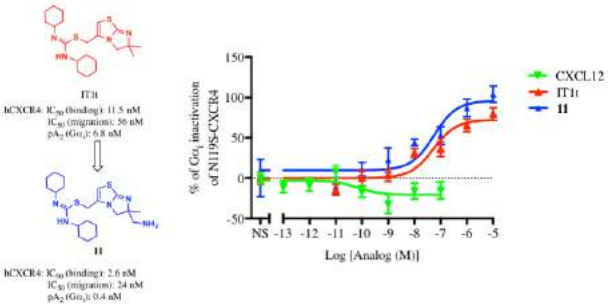

An amino functionalized analog of the CXCR4 ligand IT1t is of higher affinity and inverse agonistic potency on CXCR4-CAM receptor N119S than IT1t.

INTRODUCTION

Chemokines and their family of receptors[1] mediate several cellular functions; they are key players to initiate and direct cell movement, an essential event in embryogenesis, hematopoiesis and angiogenesis.[1] CXCL12 and its cognate chemokine receptors CXCR4 and also CXCR7[2] have been implicated in a variety of essential physiological and pathophysiological processes. Besides their normal physiological roles, they participate in inflammatory diseases[3,4] such as rheumatoid arthritis,[5] HIV infection,[6,7] cancer dissemination[8] and the WHIM syndrome (Warts, Hypogammaglobulinemia, Immunodeficiency, and Myelokathexis),[9,10] prompting to develop novel pharmacological entities to modulate or repress their functions.[11]

CXCL12 behaves as a CXCR4 agonist on several signaling pathways,[12] like the Gi/o and β-arrestin pathways,[13] regulates the retention of hematopoietic stem cells and progenitor cells in the bone marrow niche.[14] Therefore, the development of synthetic CXCR4 agonists is of great relevance for the mobilization of hematopoietic stem cells, since this approach could sidestep the use of antagonist, which leads to harmful unwanted effects in long-term use.

CXCR4 is quite pertinent in cancer and to date more than 23 types of cancer have been shown to overexpress the CXCR4.[15] Such CXCR4-positive cancer cells profit from this expression,[16] metastasize rapidly and are homing towards tissues highly expressing CXCL12[17] (i.e. lymph nodes and liver) and the bone marrow which then support their survival and protect these cancer cells from chemotherapeutic agents.

Owing to the pivotal role of this chemokine couple[18] CXCL12 and CXCR4 in the spread and progression of different types of cancer, targeting the CXCL12/CXCR4 axis could be critical for metastatic phenotypes[19] and could have a major impact on the chemotherapy potential on metastases [20] or even cancer stem cells.[21]

We recently reported the discovery and characterization of a low nanomolar class of synthetic peptidic CXCR4 agonists that mobilize REH cells (pre B-lymphocytes), a leukemia cell line. [22,23] Those molecules are promising drug candidates with the potential for widespread benefits to metastatic cancer patients. However, while those compounds present great topological and pharmacological information, they do not exhibit appropriate pharmacokinetic (PK) properties.[24]

It has been extensively shown previously that the N-terminal end of CXCL12 alone is mainly responsible for the induction of chemotaxis on stem/progenitor cells and previous SAR studies on the N-terminal pharmacophore showed the importance of several residues[25] and their contribution to the activation of the signaling cascade of CXCR4 including chemotaxis.[26]

The C-terminus end of CXCL12 plays a crucial role in the initial recognition of the chemokine receptor[27] and is particularly important for stabilization of the interactions between CXCR4 and CXCL12.[28]

Throughout electrostatic interactions with negatively charged residues from the N-terminal tail of CXCR4, the C-terminus of CXCL12 controls potency[29] and contributes to regulate CXCL12 orientation.[30]

Based on both this two-step interactions model of the CXCR4/CXCL12 couple where only the N-terminus of CXCL12 leads to conformational change allowing therefore activation of the intracellular signaling pathways of CXCR4,[31] we aimed to develop a new scaffold to design more stable agonists through structure-based drug design.

Pharmacological studies on a new class of orally bioavailable, highly potent CXCR4 antagonists and crystallographic structural studies have highlighted the potential of IT1t[32] as a scaffold (**Scheme 1**) for agonists design.[33]

On this background, we set out to develop highly potent chemotactic CXCR4 agonists with improved biopharmaceutical properties by anchoring an improved CXCL12 N-terminus peptide onto a functionalized IT1t scaffold.

RESULTS

Chemistry of novel IT1t-like molecules

In the course of SAR studies on the IT1t molecule and based on the literature, we attempt to modify the gem-dimethyl in the beta position of the endocyclic isothiourea. We substituted one of the two methyl groups with either an amino or a guanidino function, in order to insert a functional amino group for future CXCL12 N-terminus peptide anchoring.

Herein, we describe the synthesis and characterization of novel IT1t-like molecules.

The incorporation of an aminomethyl group posed synthetic challenges. As a potentially general route for exploration, we first envisioned a synthetic route starting the synthesis of a functionalized protected triamine. Our attempts focused on the formation of a suitable triamine on which the endocyclic thiourea ring could be constructed. As such, the first successful synthetic route to racemic **6** is outlined in Scheme 1 with the formation of a key target intermediate functionalized protected triamine. This synthesis favors the use of stable intermediates compared to the use of propellants (polynitro or polyazido) usually described in the literature for different polyamines.[34,35] We also avoided high pressure, high temperature hydrogenation and provided a more secure way to generate the polynitrogenated intermediate.[36] Thus, the functionalized protected triamine was formed by reaction of commercially available methyl methacrylate with freshly prepared N-tosyliminobenzyliodinane. The aziridine ring formed was converted in the intermediate **2** with two hidden amino functions. Addition of tosyl chloride fully protected the residual free amino group. Reduction of the amide group followed by protection of the resulting amine gave the key intermediate **6**, which after Birch reduction gave racemic mono-protected triamine **7**. The addition of carbon disulfide afforded the cyclic thiourea **8** in a 51% yield (2 steps). The formation of the second 5-membered ring was achieved with 1,3 dichloroacetone in acetonitrile under reflux,

providing alkyl chloride **9**. The penultimate intermediate was obtained via nucleophilic substitution with dicyclohexylthiourea using Finkelstein reaction *in situ*. Deprotection of the protected amine bis isothiourea gave the final product **11**, with an overall yield of 6.5% (**Scheme 2**).

Compound **11** was guanidinylated using Goodman reagent, followed by successive deprotection under acidic conditions (**Scheme 2**).

Compound **11** and its guanidinylated (**12**) analog were characterized via 1D- and 2D-NMR experiments and their biological activity assessed using several assays.

Biological characterization of IT1t-like molecules

Binding affinities for human CXCR4 receptor were determined by inhibition of ^{125}I-CXCL12 binding in HEK293 membranes stably expressing the human HA-tagged CXCR4 receptor as previously described.[22] Each compound was tested in an 8-point curve radioligand-binding assay to determine its IC_{50} value.

The competition curves of specific binding to human CXCR4 receptor obtained for compound **11** and IT1t show that compound **11** possesses a better binding profile than IT1t with a IC_{50} of 2.6 ± 0.06 nM (**Figure 1**) compared to 11.5 ± 1.8 nM for IT1t. Knowing that compound **11** is a racemic mixture, it is probable that only one of the two enantiomers possesses higher affinity.

In the CXCR4-IT1t complex described by Wu and coworkers,[33] the gem-dimethyl of IT1t seems to be in close proximity with Glu288$^{7.39}$ (Ballesteros-Weinstein numbering)[37] from the TMD7 of hCXCR4, which is also implicated in a salt bridge with the protonated imidazothiazole. Since the insertion of a positive charge increases potency and efficacy, it could be conceivable that the amino group from compound **11** forms an additional salt bridge within the binding pocket. 2 ns molecular dynamics (MD) simulations suggest one of the isomers of compound **11** could form an additional

salt bridge with the side-chain of residue D288$^{7.39}$, but rarely short enough to form a direct H-bond (4.8 ± 0.7 Å) (**Figure 2, A**). A water-mediated H-bond was observed (not shown). The simulation of the other isomer indicates it could form an H-bond with the sidechain of residue D187^{ECL2} (**Figure 2, B**).

The presence of localized charge seems to be preferred over charged bidentate guanidinium, as the guadininium compound (**12**) showed no affinity gain with an IC_{50} of 9.1 ± 2.9 nM. MD simulations of the two isomers of compound **12** suggest that with one of them, the guanidinium does not form additional interactions with the receptor and rather interacts with water molecules within the binding pocket (**Figure 2, C**). With the other enantiomer, the guanidinium could form new H-bonds with D171$^{4.60}$, H113$^{3.29}$ and T117$^{3.33}$ but the H-bond between the imidazothiazole and D288$^{7.39}$ is lost (**Figure 2, D**). Based on MD simulations and the first set of separated peptide conjugates (see below), we speculate that one of the isomers of **11** (most likely that presented in **Figure 2, B**) should possess a higher affinity. Regarding **12**, our model suggests different binding poses, which should translate in different affinities. However, given that both isomers make H-bonds with the receptor in their respective poses, it is difficult to predict which complex would be the most stable.

We first tested our molecules into agonist mode on both $G\alpha_i$ activation (**Figure S1, A**†) and β-arrestin-2 recruitment (**Figure S1, B**†) to ensure that the introduction of a functional charge did not induce any agonist behavior. As expected, no agonistic behavior was detected in this assay paradigm for IT1t, **11** and **12**. We then determined whether these newly synthesized molecules could act as functional antagonists on CXCR4. Receptor antagonism was determined by measuring inhibition of $G\alpha_i$ recruitment in HEK293 transiently transfected with $G\alpha_i$-91-RlucII, $G\beta_1$, and GFP^{10}-$G\gamma_1$. Cells were incubated with fixed concentrations of antagonists between 10 and 100 nM

before stimulation with increasing concentrations of CXCL12 (ranging from 10^{-13} to 10^{-7} M). The ability of our newly synthesized IT1t-like molecules to inhibit the $G\alpha_i$ response induced by CXCL12 was monitored and quantified. IT1t, **11** and **12** inhibited the $G\alpha_i$ response induced by CXCL12, however compound **11** shifted the response at significantly lower concentrations. Values of pA_2 extrapolated using the Schild/Gaddum equation were found to be 6.8 ± 2.3 nM for IT1t, 0.4 ± 0.3 nM for **11** and 8.2 ± 3.1 nM for **12**. As chemotaxis is one of the most important properties of the chemokine family, we tested the ability of these new molecules to antagonize CXCL12 action on a physiological assay, CXCL12-triggered cell migration.

Chemotaxis is a complex physical process that depends on both the physicochemical properties of the chemoattractant and the stability of the system's established gradient.[38] To fully characterize our ligands, inhibition of CXCL12-induced chemotaxis was assessed with pre-B lymphocytes (REH cells) in transwell migration assays. When assessing antagonist activity, 1 nM of CXCL12 was placed in the bottom chamber, and antagonist at increasing concentrations was placed in the same compartment as CXCL12. IC_{50} values were found to be 55.9 ± 17.3 nM, 23.6 ± 7.1 nM, and 34.7 ± 11.5 nM for IT1t, **11** and **12**, respectively (**Figure 3**).

During the above functional tests, we observed a slight increase of the BRET signal in the $G\alpha_i$ assay (**Figure S1, A**†); this could be related to a reduction of the basal activity of the CXCR4 receptor and led us to believe that the new compounds may act as inverse agonists rather than neutral antagonists.

To test this hypothesis, we used the previously reported CXCR4 constitutively active mutant (CAM), N119S,[39] for validation, with the largely described inverse agonist T140[39,40] as a positive control. Our results showed indeed a decrease in the constitutive activity in both the $G\alpha_i$ (**Figure 4, A**) and β-arrestin (**Figure 4, B**) assays, thus validating the fact that those ligands behave, in fact,

as inverse agonists. Potency to reverse the basal $G\alpha_i$ activity of the CAM receptor were found to be 11.3 ± 4.0 nM, 53.0 ± 31.1 nM, 55.7 ± 39.3 nM and 6.22 ± 4.61 nM for T140, IT1t, **11** and **12** respectively. Interestingly, compound **11** was found to be as efficient as T140 with an E_{max} of 103 ± 9 % whereas IT1t and compound **12** were only able to reverse the CAM activity of 77.0 ± 8.8 % and 80.6 ± 9.2, respectively.

Similar behavior was found on β-arrestin-2 recruitment with EC_{50} for T140, IT1t, **11**, and **12** of respectively 0.33 ± 0.31 nM, 1.51 ± 1.60 nM, 0.26 ± 0.29 nM, and 3.05 ± 2.73 nM. Surprisingly, all the compounds were found to be as efficient as T140 to reverse the CAM activity on β-arrestin-2 recruitment.

Altogether, these data confirm that analog **11** is a new potent CXCR4 inverse agonist with an interesting functional group for peptide anchoring.

It is not surprising that IT1t and IT1t-like molecules acts as inverse agonists since it was reported that 85% of reported neutral antagonists are in fact inverse agonists[41] when tested on CAM receptor or on receptor with basal activity.

Since CXCR4 plays a crucial role in the WHIM syndrome[9,10] which is associated to an increased basal CXCR4 signaling activity, IT1t and IT1t-like molecules could be a great asset for drug discovery in this particular disease.

C-terminal attachment of CXCL12 N-terminus on analog 11

Fully characterized compound **11** on biological assays was then attached on resin on the C-terminus of an immobilized CXCL12 N-terminus decapeptide (**Scheme 3**).

To do so, we used a non-conventional strategy with Ellman's DHP resin[42,43] to anchor compound **11** onto CXCL12 N-terminus peptide. First, through side chain attachment, we coupled the

dipeptide Fmoc-*L*-Ser(OH)- *L*-Ala-OAllyl (**14**) under microwave irradiation, then elongated the peptide using standard Fmoc/t-Bu SPPS to obtain the decapeptide protected on its C-terminal by an allyl ester. After stepwise solid-phase peptide synthesis, the decapeptide was deprotected on its C-terminus using palladium and phenylsilane, then **11** was coupled using HATU and DIPEA. The target compounds were obtained in a 1/1 diastereoisomeric mixture that was separated by HPLC afterwards.

We first examined the binding properties of both diastereoisomers on the human CXCR4 receptor. IC_{50} values were found to be 0.49 ± 0.13 nM for CXCL12, 334 ± 67 nM for compound **16** and 111 ± 20 nM for compound **17** (**Figure S2**†), thus exhibiting a loss of affinity of nearly 30- and 10-fold for compounds **16** and **17**, respectively.

Biological studies were done using the $G\alpha_i$ activation assay in the agonist paradigm. Cells were stimulated with increasing concentrations of compounds **16** and **17** (10^{-11} to 10^{-5} M) and we monitored the ability of these compounds to activate $G\alpha_i$. Despite their agonist moiety, both diastereoisomers failed to induce $G\alpha_i$ response at concentrations up to 10^{-5}M (**Figure S3**†).

Since cell migration was shown to be an integrative pathway involving multiple downstream activation cascades, we then performed Transwell migration assay in the agonist paradigm to observe whether compounds **16** and **17** could activate other pathways than the $G\alpha_i$ pathway. Unfortunately, those compounds were not able to trigger any migration of REH cells (**Figure S4**†).

In the light of these results, we performed the same assays in an antagonist paradigm to investigate whether our compounds behaved as antagonists and were able to inhibit the $G\alpha_i$ response induced by CXCL12 as well as the CXCL12-triggered migration of REH cells. In the $G\alpha_i$ assay, compound **16** and **17** were found to be antagonists at the CXCR4 receptor with a pA2 value of 171 ± 108 nM and 85 ± 25 nM respectively. These values were higher than the pA2 value of **11** alone. This

antagonist behavior was also found in the migration assay were both compounds **16** and **17** inhibited CXCL12-induced migration with an IC_{50} of > 2,000 nM and 914 ± 443 nM, respectively (**Figure 5**). With the CXCR4-IT1t complex described by Wu et al., [33] and with the recent homology model with CXCL12 based on the published crystal with the viral chemokine v-MIPII,[44] highlighting the subpockets implicated in the two-step binding of CXCL12, we can observe that IT1t occupies the same region as the N-terminus of CXCL12. IT1t is involved in several interactions with charged residues of the CXCR4 receptor like Asp97$^{2.63}$ and Glu288$^{7.39}$ that occurs to interact with the N-terminus Lysine of CXCL12.[44] Since the C-terminus hybrids retain higher affinity to CXCR4 than the N-terminus decapeptide of CXCL12[26] and since compound **11** seems to behave similarly to IT1t, it is plausible that compound **11** drives the binding of the hybrids molecules **16** and **17** and places the N-terminus of CXCL12 in a mismatch position for activation.

N-terminal attachment of CXCL12 N-terminus on analog 11

In the light of these results and based on recent structural data[44] showing that IT1t occupies a similar position in the crystal than the activation responsible dipeptide Lys-Pro, [23,45] respectively in position 1 and 2 of the N-terminal chain of the CXCL12, we focused on another strategy to graft compound **11**, our most potent inverse agonist, in place of the N-terminus dipeptide Lys-Pro (**Scheme 4**). Using a bromoacetate strategy, we firstly synthesized the des-Lys-Pro N-terminus octapeptide of CXCL12 using Rink Amide resin.

When the stepwise solid-phase peptide synthesis was completed, the octapeptide N-terminal was deprotected with piperidine in DMF. Simultaneously, we freshly prepared the symmetric 2-bromoacetic anhydride using bromo acetic acid and N,N-Diisopropylcarbodiimide (DIC). Simple addition of the anhydride mixture onto the resin with stirring for 30 minutes provided the bromo

intermediate, subsequent SN2 substitution with compound **11** and DIPEA provided the pure diastereoisomeric mixture of N-terminus modified hybrids (Compound **18**).

Pharmacodynamic studies were assessed using the same assays as previously described in agonist mode. Firstly, we assessed the binding affinity of compound **18**. This C-terminus hybrid binds with an IC_{50} of 22.2 ± 1.6 nM (**Figure S5**†).

$G\alpha_i$ recruitment using BRET-based assays showed no activation whatsoever of the CXCR4 receptor (**Figure S6**†). We then performed Transwell migration assays and observed that this hybrid was not able to induce REH chemotaxis (**Figure S7**†).

In the light of these results, we performed the same assays in an antagonist paradigm to investigate whether compound **18** behaved as an antagonist and was able to inhibit the $G\alpha_i$ response induced by CXCL12 as well as the CXCL12-triggered migration of REH cells. In the $G\alpha_i$ assay, compound **18** was found to be an antagonist at the CXCR4 receptor with a pA2 value of 8.51 (3.07 ± 2.2nM), this value was found to be closer to the pA2 of the value of **11** alone (**Figure S8**†).

The reverse attachment of CXCL12 N-terminus on compound **11** led to a significantly increase of affinity which tends to support that the N-terminus of CXCL12 may be placed in a more optimized position in the receptor. However, since no activity was observed, the hybrid seems to block the CXCR4 receptor in an energy minimum stabilizing an inactive state of the receptor (**Figure S9**†). Furthermore, it has been shown that Lys^1 of CXCL12 is highly important for the activation of $CXCR4^{46}$ and as compound **11** seems to occupy the same binding pocket,[44] it is likely that compound **11** may block the activation hot spot and that the hybrid is behaving like analog **11**. Furthermore, our recent works suggest that Lys^1 of CXCL12 breaks the interaction between $D288^{7.39}$ and $Y116^{3.32}$, leading to an increased separation between TMD3 and TMD7 through an interaction of its ε-NH_3 with the side chain of $Y116^{3.32}$ and its N-terminus with $D288^{7.39}$. We believe

a hybrid molecule that leads to similar interactions, possibly with the CXCL12 N-terminus-derived moiety forming a salt bridge with D288$^{7.39}$ while the imidazothiazole of IT1t interacts with Y116$^{3.32}$, could present agonistic properties[23,45]. Future experiments will focus on exploring this hypothesis.

CONCLUSIONS

Throughout this study, we have optimized a synthesis of amino- and guanidine-functionalized IT1t analogues, using a safe and robust synthesis of triamines. Very few methods are reported for the synthesis of this kind of compounds and this constitute a new versatile synthetic way for polynitrogenated compounds. Next, we revealed the inverse agonistic behaviour of IT1t and IT1t-like molecules on the CXCR4 receptor. We discovered that the insertion of a positive charge either by amino methyl or guanidino methyl gave potent inverse agonists, which opens the way for subsequent optimization of this class of molecules. Moreover, insertion of primary amine and a localized positive charge on the gem-dimethyl moiety increased the inverse agonist behavior compared to the reported IT1t. This molecule could be used as a tool to explore the structural features of the CXCR4 receptor.

We have described two types of hybridization with our compound. However, further hybrids design should be done to use analog **11** as a scaffold for agonist design.

EXPERIMENTAL SECTION

Synthetic procedures

Reagents were purchased from Sigma Aldrich. Solvents were purchased from Fischer and used as received. Reactions were carried out under inert atmosphere of dry argon in oven-dried glassware. Reactions were monitored using thin-layer chromatography (TLC).

TLC was performed on glass plates SIL 60 G-25, UV254, 0.25mm, 20 x 20 cm (Canadian Life Science, Peterborough, ON).

Amino acids, TFA and DIPEA were purchased from Chem-Impex. DMF was stored over 3Å molecular sieves. Peptide synthesis was performed in 6 mL polypropylene cartridge with 20µm PE frit from Applied Separations (USA). Peptides were shaken (~180 rpm) on a New Brunswick Scientific orbital shaker.

Preparative purifications were made on a Waters preparative HPLC system paired with an ACE 5 C18 column. Analytical HPLC were performed on a Water H Class Acquity UPLC coupled with a SQ Detector 2 and a PDA eλ detector and paired with a Acquity UPLC BEH C18 column, 1.7µm, 2.1 x 50 mm. Diastereoisomer separation was assessed on a Waters Mass-trigggered preparative HPLC system paired with a x-SELECT CSH Prep C18 5µm column coupled with a SQ Detector 2 and a PDA eλ detector.

Chromatography and MS spectra were recorded on a Waters UPLC-MS system, and compounds were dissolved in a mixture of acetonitrile and 0.1% TFA in water.

NMR spectra were recorded in deuterated solvents on a Bruker AC300 NMR or a Varian 300 NMR or a Varian 600. NMR chemical shifts are reported in ppm (parts per million) and coupling constants (J) in Hertz. The abbreviations for peak multiplicities are described as follows: s (singlet),

d (doublet), dd (doublet of doublets), t (triplet), q (quartet), qt (quintet), m (multiplet) and bs (broad singlet).

2D experiments were performed on a Varian 600 MHz spectrometer equipped with a Z-axis pulsed-field gradient triple resonance probes.

HRMS were performed on a Bruker MaXis 3G high resolution Q-ToF.

Synthesis of (Z)-(6,6-dimethyl-5,6-dihydroimidazo[2,1-b]thiazol-3-yl)methyl N,N'-dicyclohexylcarbamimidothioate or IT1t.

Synthesis of IT1t was done according to the paper of Thoma et al.

Synthesis of N-tosyliminobenzyliodinane[47] **(**Compound **1)**

To a cooled suspension (temperature below 10 ˚C) of p-toluenesulfonamide (20.52 g), potassium hydroxide (16.80 g) and dry methanol (500 ml) under stirring was added iodobenzene diacetate (38.4 g) by portions. The resulting yellow colored solution was allowed to warm to room temperature and then stirred for 3 h. 300 mL of iced water was poured into the reaction mixture and the light yellow suspension was stirred overnight. The light yellow solid was isolated by filtration and filtered on a Büchner funnel. The solid was washed with ether at least three times (3x 100 mL) to remove residual iodobenzene then dissolved in boiling methanol (150 mL) and recrystallized in a freezer overnight. A pale yellow solid was then obtained by filtration. Yield 81% (36.2g recovered).

^{1}H NMR (300MHz, DMSO-d_6): δ 7.69 (d, 2H), δ 7.45 (m, 3H), δ 7.3 (m, 2H), δ 7.05 (d, 2H), δ 2.27 (s, 3H)

^{13}C NMR (300MHz, DMSO-d_6): δ142.6, 142.1, 137.8, 131.4, 130.1, 128.5, 126.3, 128.1, 126.3, 95.6, 21.7

Synthesis of methyl 2-methyl-1-tosylaziridine-2-carboxylate[48] **(**Compound **2).**

To a solution of dry acetonitrile (120 mL), molecular sieves 4Å (8.4 g) and $Cu(OTf)_2$ (1.01 g, 0.1 eq., 2.79 mmol) under stirring was added methyl methacrylate (3 mL, 1 eq., 28.17 mmol) and by portions PhINTs (1) (12.63 g, 1.2 eq., 33.86 mmol).

The reaction mixture was stirred at room temperature overnight.

The pale green crude solution was filtered on a pad of silica, and then washed in a hexane-ethyl acetate mixture (1:1). The filtrate was evaporated to dryness to give a brown oily solution, which was then purified by flash chromatography using ethyl acetate-hexane (30:70).

The desired product was obtained as an off white crystal.

Yield: 78% (6.7 g)

^{1}H NMR (300MHz, DMSO-d_6): δ 7.78 (d, 2H, J=8.1Hz), δ 7.46 (d, 2H, J=8.0Hz), δ 3.65 (m, 3H,), δ 2.79 (d, 2H, J=7.5Hz), δ 2.41 (s, 3H), δ 1.73 (s, 3H)

^{13}C NMR (300MHz, DMSO-d_6): δ 167.6, 143.8, 135.8, 129.2, 126.4, 52.1, 45.6, 20.3, 14.3

MS (ES+) m/z $(M+H)^+$ 270.78 $(M+Na)^+$ 292.76

Synthesis of 3-amino-2-methyl-2-(4-methylphenylsulfonamido)propanamide (Compound **3)**.

Methyl 2-methyl-1-tosylaziridine-2-carboxylate (4.5 g, 16.7 mmol) of compound **2** was dissolved in ammonia (7M in methanol, 20 eq., 40 mL)[49]. The mixture was heated in a sealed tube at 65 ˚C overnight. After cooling to room temperature, the solvent was removed under vacuum and the crude product used in the next step without further purification (mean conversion: 85%).

^{1}H NMR (300MHz, DMSO-d_6): δ 7.73 (d, 2H, J=8.2Hz), δ 7.36 (d, 2H, J=8.1Hz), δ 7.17 (d, 2H, J=10.1Hz), δ 3.65 (bs, 2H), δ 3.34 (bs, 2H), δ 2.65 (dd, 2H, J=13.5Hz), δ 2.37 (s, 3H), δ 1.10 (s, 3H)

^{13}C NMR (300MHz, DMSO-d_6): δ 174.6, 142.2, 140.6, 129.3, 126.2, 63.0, 49.5, 20.9, 19.8

Synthesis of 2-methyl-2,3-bis(4-methylphenylsulfonamido)propanamide (Compound **4).**

To a slurry of 3-amino-2-methyl-2-(4-methylphenylsulfonamido)propanamide (4.53 g, 16.7 mmol) in water (40 mL) was added NaOH (0.4 g, 0.6 eq., 10 mmol) to adjust the pH to 10 followed by dropwise addition of a solution of *p*-toluenesulfonyl chloride (3.80 g, 1.2 eq., 20.04 mmol) in acetone (10 mL) simultaneously with NaOH (0.4 g, 0.6 eq., 10 mmol) to maintain a pH of 10. The reaction mixture was heated at 45 ˚C for one hour and once the starting material was consumed; the pH was adjusted to 2-3 with 6M HCl.

The reaction mixture was then extracted with ethyl acetate (3x80 mL), the organic phases washed with brine (3x40 mL) then pooled, dried with dry $MgSO_4$ and concentrated under vacuum.

The oily residue was dissolved in ethyl acetate to perform a solid deposit and then, the crude product was purified by flash column chromatography using ethyl acetate: hexane (90:10). The desired product was obtained as a bright white crystal. Yield: 71% (5.03 g)

^{1}H NMR (300MHz, DMSO-d_6): δ 7.68-7.59 (m, 4H), δ 7.40-7.31 (m, 6H), δ 7.20 (d, 2H, J=16.1Hz), δ 2.83 (s, 2H), δ 2.39 (s, 3H), δ 2.37 (s, 3H), δ 1.16 (s, 3H)

^{13}C NMR (300MHz, DMSO-d_6): δ 174.0, 146.6, 143.4, 141.1, 138.2, 130.5, 130.3, 127.4, 127.3, 62.1, 50.7, 21.9, 20.6

Synthesis of N,N'-(3-amino-2-methylpropane-1,2-diyl)bis(4-methylbenzenesulfonamide) (Compound **5).**

Borane tetrahydrofuran complex (1M solution in THF, 18.8 mL, 2 eq., 18.8 mmol) was added to a round-bottom flask containing 2-methyl-2,3-bis(4-methylphenylsulfonamido)propanamide (4 g, 9.4 mmol) at 0 ˚C. The reaction mixture was kept at 0°C until hydrogen evolution stopped, then refluxed overnight. After cooling to room temperature, the solvent was removed under vacuum and the crude product was co-evaporated at least three times with methanol. Completion was checked by UPLC-MS and the crude product was used directly in the next step without further purification (Conversion rate: 99%).

Synthesis of tert-butyl (2-methyl-2,3-bis(4-methylphenylsulfonamido)propyl)carbamate (Compound **6).**

To a stirred mixture of tert-butyl (2-methyl-2,3-bis(4methylphenylsulfonamido)propyl) carbamate (3.87 g, 9.4 mmol) and triethylamine (5 mL, 4 eq., 37.6 mmol) in DCM (40mL) was added di-*tert*-butyl dicarbonate (4.10 g, 2 eq., 18,8 mmol). The resulting solution was stirred at room temperature for at least 3 hours. The reaction was monitored by TLC until completion.

Once completed, the reaction mixture was extracted with ethyl acetate, the organic phases washed with HCl 1M and brine then gathered, dried with dry $MgSO_4$ and concentrated *in vacuo*.

The oily residue was dissolved in DCM to perform a solid deposit, then the crude product was purified by flash column chromatography using ethyl acetate: hexane (1/1). The desired product was obtained as a white powder. Yield: 73% (3.5 g)

^{1}H NMR (300MHz, $CDCl_3$): δ 7.72 (dd, 4H, J=8.6Hz, J=6.4Hz), δ 7.29 (m, 4H), δ 5.37 (t, 1H, J=7.6Hz), δ 5.31 (s, 1H), δ 3.97 (dd, 2H, J= 11.4Hz), δ 2.95 (m, 2H), δ 2.42 (d, 6H, J=3.3Hz), δ 1.43 (s, 9H), δ 1.14 (s, 3H)

^{13}C NMR (300MHz, $CDCl_3$): δ 153.2, 143.5, 143.4, 139.4, 136.5, 129.7, 129.6, 126.9, 126.8, 83.1, 69.6, 57.8, 48.5, 27.5, 21.4, 19.3

Synthesis of tert-butyl (2,3-diamino-2-methylpropyl) carbamate (Compound **7).**

The Birch reaction was conducted in a three-necked round-bottom flask with a dry ice condenser, a gaseous NH_3 inlet and a stopper for sodium addition, using THF freshly distilled over sodium and benzophenone. Ammonia (90 mL) was condensed at -78 ˚C then Na (1.8 g, 20 eq., 7.83 mmol) was added and the solution turned immediately dark blue. A solution of (**6**) (2 g, 3.91 mmol) in dry THF (12 mL) was added to the reaction mixture.

After consumption of the starting material (not detectable after 1 h by UPLC-MS and TLC), the unreacted Na was quenched with a mixture of THF/Methanol (1/1) (30 eq. of Methanol, 4,75 mL) until discoloration of the mixture. Upon discoloration, ammonia was evaporated under a flow of air, until the pH of the airflow was neutral. The reaction mixture was then dissolved in water until complete dissolution of precipitate then evaporated *in vacuo*. The resulting aqueous phase (acidified to a pH around 6-7 with HCl 1M) was extracted with ether (5x 15 mL). The aqueous phase was lyophilized and the following reaction was started without further purification

MS (ES+) m/z $(M+H)^+$ 204.85

Synthesis of tert-butyl ((4-methyl-2-thioxoimidazolidin-4-yl) methyl) carbamate (Compound **8).**

A solution of the above crude materials containing *tert*-butyl (2,3-diamino-2-methylpropyl) carbamate (794 mg, 1 eq., 3.89 mmol) in DCM (20mL) was cooled down to 0 ˚C then carbon disulfide (520 µL, 2.2 eq., 8.56 mmol) was slowly added[50]. The reaction mixture was refluxed overnight. Once completed, the solvent was evaporated and the oily residue purified by flash chromatography from DCM 100% to DCM-Methanol (98: 2). The desired product was obtained as a pale yellow powder. Yield: 51% for 2 steps (489 mg)

^{1}H NMR (300MHz, DMSO): δ 7.98 (d, 2H, J=14.2Hz), δ 6.94 (t, 1H, J=5.5Hz), δ 3.43-2.95 (m, 4H), δ 1.37 (s, 9H), δ 1.11 (s, 3H)

^{13}C NMR (300MHz, DMSO): δ 179.8, 154.5, 76.4, 61.0, 51.7, 45.5, 26.6, 21.9

Synthesis of tert-butyl ((4-methyl-2-thioxoimidazolidin-4-yl)methyl)carbamate (Compound **9).**

A solution of *tert*-butyl ((4-methyl-2-thioxoimidazolidin-4-yl)methyl)carbamate (186 mg, 1 eq., 0.76 mmol), 1,3-dichloro acetone (161 mg, 0.9 eq., 1.27 mmol) and acetonitrile (2 mL) was refluxed for 4 hours[50]. The reaction was monitored by UPLC-MS. Once completed, the crude was basified with saturated $NaHCO_3$ to a pH around 7-8 then extracted three times with ether (3*4 mL). The organic layer was washed with brine, dried over dry $MgSO_4$ and concentrated *in vacuo.* The product was then dried overnight *in vacuo*. The product was used without further purification with a mean purity of 80%. Yield: 80% (192 mg). Purity: 80% (UPLC-UV).

^{1}H NMR (300MHz, DMSO): δ 6.86 (t, 1H, J=5.7Hz), δ 6.14 (s, 1H), δ 4.54 (dd, 2H, J=12.3Hz), δ 3.65 (dd, 2H, J= 9.5Hz) δ 2.99-3.16 (m, 2H), δ 1.40 (s, 9H), δ 1.21 (s, 3H)

^{13}C NMR (300MHz, DMSO): δ 166.3, 156.5, 132.4, 102.8, 78.2, 53.9, 48.8, 37.7, 28.6, 25.7

Synthesis of (Z)-tert-butyl ((3-(((N,N'-dicyclohexylcarbamimidoyl)thio)methyl)-6-methyl-5,6-dihydroimidazo[2,1-b]thiazol-6-yl)methyl) carbamate (Compound **10).**

To a solution of *tert*-butyl ((4-methyl-2-thioxoimidazolidin-4-yl)methyl) carbamate (100 mg, 1 eq., 0.31 mmol) in acetone was added TBAI (30 mg, 0,25 eq., 0.079 mmol) followed by K_2CO_3 (136 mg, 3 eq., 0.95 mmol) and dicyclohexylthiourea (78 mg, 1 eq., 0.31 mmol). The reaction mixture was then heated at 55 ˚C for 1 hour and monitored by UPLC-MS. After consumption of the starting material, the crude was evaporated then dissolved in DCM and washed with citric acid 1M. The aqueous phase was concentrated *in vacuo* and the product purified by preparative HPLC. The compound was purified at a 230 nm wavelength using a 10-45% gradient of acetonitrile with 0.1% TFA. Yield: 30%

^{1}H NMR (300MHz, DMSO): δ10.40 (bs, 2H), 9.29 (bs, 2H), δ 7.30 (t, 2H, J=8.4Hz), δ 6.84 (s, 1H), δ 4.59 (dd, 2H, J= 15.2Hz), δ 4.25 (dd, 2H, J=11.1Hz), δ 3.74 (bs, 2H), δ 3.34 (m, 3H), δ 2.79 (m, 2H), δ 1.85-1.05 (m, 20H), δ 1.45 (s, 3H), δ 1.39 (s, 9H)

^{13}C NMR (300MHz, DMSO): δ 149.9, 141.5, 137.2, 112.1, 91.4, 59.4, 53.5, 37.3, 35.9, 34.0, 28.5, 13.1, 12.0, 9.1, 5.4, 4.5

MS (ES+) m/z $(M+H)^+$ 523.0

HRMS: m/z calculated for $C_{26}H_{43}N_5O_2S_2$: m/z calculated 522.2931 (MH^+), m/z observed: 522.2952 (MH^+).

Synthesis of (Z)-2-((6-(ammoniomethyl)-6-methyl-5,6-dihydroimidazo[2,1-b]thiazol-3-yl)methyl)-1,3-dicyclohexylisothiouronium (Compound **11).**

To a solution of (**10**) (49 mg, 0.094 mmol) was added hydrogen chloride solution 4 M in dioxane (4 eq., 95 µL, 0.38 mmol). The reaction mixture was stirred for 30 minutes, then the product precipitated in ether. The resulting precipitate was dissolved in water and dried under vacuum to remove the residual traces of ether, then lyophilized. If the product was not purified at the previous step then the aqueous phase was purified on a preparative HPLC system at 232 nm and 260nm using a 5-30% gradient of acetonitrile with 0.1% TFA.

All fractions containing the desired product were lyophilized and analyzed by UPLC-MS in a in a 50mM ammonium formate buffer.

^{1}H NMR (300MHz, DMSO): δ 9.27 (bs, 2H), δ 8.42 (bs, 3H), δ 6.87 (s, 1H), δ 4.60 (dd, 2H, J= 15.3Hz), δ 4.34 (dd, 2H, J= 11.7Hz), δ 3.74 (bs, 2H), δ 3.28 (dd, 2H, J= 14.4Hz), δ 1.83-1.06 (m, 20H), δ 1.57 (s, 3H)

^{13}C NMR (300MHz, DMSO): δ 169.3, 160.9, 158.7, 156.6, 131.5, 110.8, 78.8,72.9,56.7, 55.2, 53.4, 47.9,32.5, 31.4, 28.5, 24.8, 23.9

HRMS: m/z calculated for $C_{21}H_{35}N_5S_2$: m/z calculated 422.2407 (MH^+), m/z observed: 422.2409 (MH^+).

Synthesis of ((Z)-(6-(guanidinomethyl)-6-methyl-5,6-dihydroimidazo[2,1-b]thiazol-3-yl)methyl N,N'-dicyclohexylcarbamimidothioate (Compound **12).**

To a solution of (**11**) (30 mg, 1 eq., 0.07 mmol) in DCM (2 mL) was added Et_3N (2 eq., 24 µL, 0.14 mmol) followed by Goodman reagent [51](1 eq., 24 mg, 0.07 mmol). The mixture was stirred at r.t. for 4 hours. After completion, DCM was evaporated and the mixture was diluted with water and purified on a mass-triggered preparative HPLC system using a 5-20% gradient of acetonitrile

with 0.1% formic acid. All the fractions containing the desired product were lyophilized and analyzed by UPLC-MS and NMR.

^{1}H NMR (300MHz, DMSO): δ 9.29 (d, 4H, J=25.6Hz), δ 8.48 (t, 1H, J=6Hz), δ 7.63 (bs, 3H), δ 7.39 (s, 1H), δ 6.90 (s, 1H), δ 4.65 (dd, 2H, J=15.1Hz), δ 4.28 (dd, 2H, J=11.3Hz), δ 3.79-3.55 (m, 9H), δ 1.85-1.09 (m, 21H), δ 1.55 (s, 3H)

^{13}C NMR (300MHz, DMSO): δ 169.9, 161.2, 159.3, 159.1, 158.2, 131.5, 118.6, 116.6, 111.4, 72.4, 56.9, 55.0, 53.7, 48.4, 32.7, 32.7, 31.6, 29.1, 28.3, 25.1, 24.9, 24.3

HRMS: m/z calculated for $C_{22}H_{37}N_7S_2$: (MH^+) 464.2625, m/z observed: (MH^+) 464.2630.

Synthesis of (S)-allyl 2-((S)-2-((((9H-fluoren-9-yl)methoxy)carbonyl)amino)-3-(tert-butoxy)propanamido)propanoate (Compound **13).**

In a 35 mL microwave vial equipped with a magnetic stir bar, L-Alanine allyl ester hydrochloride (500 mg, 1 eq, 3.87 mmol) was dissolved in DMF (15 mL), followed by DIPEA (4.05 mL, 6 eq, 23.22 mmol). After complete dissolution, Fmoc-O-*tert*-Butyl-L-serine (2.37 g, 1.6 eq, 6.19 mmol) was added to the reaction mixture followed by HATU (2.35 g, 1.6 eq, 6.19 mmol) and HOAt (843 mg, 1.6 eq, 6.19 mmol). The mixture was subjected to MW irradiation (CEM Discover Microwave S-Class) three times for 28 minutes at 40W and at 50 ˚C.[52] The reaction mixture was then poured on ice in an Erlenmeyer flask followed by 3 mL of water. The suspension was further filtered on a Büchner funnel. The precipitate was washed three times with water then dissolved in ethyl acetate, dried over anhydrous magnesium sulfate, filtered then evaporated.

The oily residue was dissolved in methanol to perform a solid deposit, then the crude product was purified by flash column chromatography using ethyl acetate: hexane (wavelengths: 264nm and 254nm). Yield: 60% (1.15 g)

^{1}H NMR (300MHz, DMSO): δ 7.50 (d, 2H, J=7.5Hz), δ 7.34 (d, 2H, 7.2Hz), δ 7.133 (d, 2H, J=7.5Hz), δ 7.04 (d, 2H, J=7.2Hz), δ 5.70- 5.56 (m, 1H), δ 5.51 (s, 1H), δ 5.09- 4.97 (m, 2H), δ 4.38-4.31 (m, 3H), δ 4.12 (d, 2H, J= 6.9Hz), δ 3.96 (t, 2H, J=6.9Hz), δ 3.57-3.54 (m, 1H), δ 3.12 (t, 1H, J= 8.4Hz), δ 1.33 (s, 2H), δ 1.17 (d, 3H, J=7.2Hz), δ 0.97 (s, 9H)

^{13}C NMR (300MHz, DMSO): δ 172.0, 169.7, 155.8, 143.5, 141.0, 131.3, 127.5, 126.8, 124.9, 119.7, 118.5, 74.2, 66.9, 65.7, 61.5, 53.9, 48.1, 46.9, 27.1, 18.2

MS (ES+) m/z $(M+H)^+$ 496.2 $(M+Na)^+$ 518.0

Synthesis of (S)-allyl 2-((S)-2-((((9H-fluoren-9-yl)methoxy)carbonyl)amino)-3-hydroxypropanamido)propanoate (Compound **14).**

1.15 g of compound **12** was dissolved in a 10 mL solution of TFA: DCM: TIPS (50: 50: 5). The reaction mixture was stirred at room temperature for 1 h. Once completed, the reaction mixture was evaporated under vacuum then extracted with ethyl acetate. The organic phase was washed with NaOH 1M until a complete neutralization of the residual TFA followed by washes with brine. The organic phase was then dried under $MgSO_4$, filtered on a Büchner funnel and concentrated under vacuum. Yield: 88% (899 mg)

MS (ES+) m/z $(M+H)^+$ 440.1 $(M+Na)^+$ 462.0

^{1}H NMR (300MHz, DMSO): δ 8.68 (d, 1H, J=6.8Hz), δ 8.38 (d, 2H, 7.5Hz), δ 7.76 (d, 2H, J=8Hz), δ 7.41 (dt, 2H, J=7.3Hz), δ 5.82- 6.00 (m, 1H), δ 5.28 (dd, 2H, J=17.2Hz, J=10.5Hz), δ 4.64- 4.55 (m, 2H), δ 4.38-4.23 (m, 4H), δ 4.16 (q, 1H, J= 6.8Hz), δ 3.94 (bs, 3H), δ 3.69-3.53 (m, 2H), δ 1.36-1.33(m, 3H)

^{13}C NMR (300MHz, DMSO): δ171.4, 169.5, 167.3, 155.3, 143.2, 140.1, 131.7, 127.0, 126.4, 124.7, 119.5, 117.0, 65.1, 64.2, 64.1, 61.1, 56.5, 47.1, 46.0, 16.3, 16.0

HRMS: m/z calculated for $C_{24}H_{26}N_2O_6Na$: 461,1683 (MNa^+), m/z observed: 461,1692 (MNa^+).

Synthesis of Nα, ε-bis-Boc-L-lysine[53] in solution (Compound **14).**

L-lysine hydrochloride (2 g, 1 eq., 10.95 mmol) was dissolved in 20 mL of water, then $NaHCO_3$ (2.76 g, 3 eq., 32.84 mmol) was added. The mixture was cooled to 0 ˚C, then Boc anhydride (2.86 g, 2 eq., 26.2 mmol) in THF was added. Then the reaction mixture was stirred at room temperature for 12 h. After 12 h, 2 equivalent of Boc anhydride were added at 0 ˚C and the mixture was stirred for an additional 12 h at room temperature. At the end of the reaction, THF was removed under reduced pressure and the aqueous layer washed with diethyl ether to remove organic impurities. The resulting aqueous layer was acidified to pH 4−5 using citric acid solution 1M then extracted with DCM. The organic layer was then washed with brine and dried with dry $MgSO_4$. The organic layer was removed under reduced pressure to obtain the compound in quantitative yield.

^{1}H NMR (300MHz, $CDCl_3$): δ 10.48 (s 1H), δ 6.26 (s, 1H), δ 5.31 (d, 2H, J= 7.8Hz), δ 4.74 (bs, 1H), δ 4.09-4.29(m, 1H), δ 3.09 (s, 2H), 1.64-1.83 (m, 6H), δ 1.43 (s, 18H)

^{13}C NMR (300MHz, $CDCl_3$): δ 176.0, 156.0, 155.6, 79.8, 79.1, 52.9, 39.9, 31.8, 29.2, 28.2, 22,2

HRMS m/z calculated for $C_{16}H_{30}N_2O_6Na$: 369.1996 ($M+Na^+$), m/z observed: 369.2009 ($M+Na^+$).

Synthesis of Ellman DHP resin[42] from Merrifield chloromethyl resin[54] for C-terminal attachment of Compound **11.**

In a round bottom flask was added NaH (60%, 1.4 g, 5 eq., 35 mmol) and THF (30 mL). The solution was cooled down to 0 ˚C then 3,4-dihydro-2H-pyran-2-ylmethanol (3.62 mL, 5 eq., 35 mmol) was added. The reaction was allowed to warm up to room temperature and stirred for 2 h. After 2 h, a thick light yellow suspension was obtained. 60 mL of dry DMF was further added to

obtain an orange opaque solution. In a 250 mL glass peptide-shaking vessel, Merrifield chloromethyl resin (5 g) was washed with DMF (60 mL) then drained followed by the addition of the orange solution. The reaction mixture was vented frequently especially during the first hour. More DMF (60 mL) was further added then the dark brown suspension was shaken at room temperature overnight. The resin was drained and washed with DCM (80 mL), DMF/water 1:1 (4x 80 mL), DMF (3x 80 mL) and DCM (3x 80 mL). The resin was briefly dried *in vacuo* and brought onto the next step as is.

Side chain attachment of (S)-allyl 2-((R)-2-((((9H-fluoren-9-yl)methoxy)carbonyl)amino)-3-hydroxypropanamido)propanoate on Ellman DHP resin.

In a 10 mL glass shaking vessel, **(***S*)-allyl 2-((*R*)-2-(((((9*H*-fluoren-9-yl)methoxy)carbonyl) amino)-3-hydroxypropanamido) propanoate was added to a solution of Ellman DHP resin (250mg). The suspension was flushed with argon and R-(-)-Camphorsulfonic acid (23mg, 0.4eq, 0.10mmol) was added. The mixture was shaken at room temperature overnight. The resin was drained and washed for 3 minutes with DCM (8 mL), IPA (8 mL), DMF (8 mL) and DCM (8 mL) (3x each). The resin was washed with ether (3x 8 mL) and dried *in vacuo* overnight.

Loading was controlled by UV measurement (λ=301nm and 290nm) of dibenzofulvene using spectrophotometer and Cuvette: Hellma 104-QS, Suprasil Quartz Z600288 10mm, 200-2500 nm (Loading= 0.3867mmol/g). Synthesis was pursued with standard Fmoc/t-Bu protected amino acids purchased from Chem Impex at the highest purity available.

Syntheses were performed using Fmoc-N-protected amino acid (3 eq.) in the presence of [O-(7-azabenzotriazol-1-yl)-1,1,3,3-tetramethyluronium hexafluorophosphate] HATU (3 equiv.), N,N-diisopropylethylamine (9 eq.) in DMF (1.5 mL) for at least 2 hours. Fmoc deprotection was

performed using 50% Piperidine in DMF for 20 minutes. Deprotection after proline coupling was performed under microwave irradiation using 2% DBU 2% Piperidine in DMF. The resin was subjected to MW-irradiation (CEM Discover Microwave S-Class) for 20 minutes at 100W and at a temperature of 75°C. After each coupling and deprotection, Kaiser test was done to monitor completion.

General procedure for allyl protecting group removal.

Dry DCM was vented under nitrogen for 30 minutes then 2 mL of DCM was added to Allyl C-terminus protected peptide. $Pd(Ph_3)_4$ (0.5 eq.) was added to the resin followed by 10 equivalents of phenylsilane. The reaction mixture was vented for a couple of minutes under nitrogen, then placed on an orbital shaker for at least 2 hours. The reactant mixture turned dark brown. After 2 hours, the resin was drained and washed with DMF (3x 3 mL) and three cycles alternatively washing with 2-propanol (3 mL) or DCM (3 mL). The resin was further washed for 3 cycles of 5 minutes with a 0.02M solution of sodium diethyl dithiocarbamate trihydrate in DMF (turning almost instantaneously pale yellow) followed by three regular cycles of washes with 2-propanol (3 mL) or DCM (3 mL). The resin was briefly dried *in vacuo* and brought on to next step as is. UPLC was used to monitor full deprotection of the C-terminus of the resin.

Standard procedure for the synthesis of the decapeptide, compound 16 and 17

Fmoc-L-Ser-L-Ala-Allyl ester DHP resin (0.3867 mmol/g, 0.1 g) was deprotected with 50% piperidine/DMF for 20 min and reacted with a Fmoc N-protected amino acid (3 eq.) in the presence of HATU (3 eq.), *N,N*-diisopropylethylamine (9 eq.) in DMF (1.5 mL) for at least 2 hours. The

resin was washed after each coupling and deprotection step by shaking 5 min in DMF (2x 3 mL) and three cycles alternatively washing 2-propanol (3 mL) or DCM (3 mL). In order to continue the synthesis of the chimeras and to anchor compound **11**, last coupling was done using Nα, ε-bis-Boc-L-lysine. N-terminus Boc protected peptides were then deprotected on their C-terminus position following the general procedure for allyl protecting group removal. Compound **11** was coupled to the peptides using HATU and DIPEA in a 1/1 proportion to avoid side reactions.

Peptides were cleaved using 95% TFA, 2.5% TIPS, 2,5% H2O for at least 2 hours to provide a mixture of diastereoisomers **16** and **17**.

The resin suspension was filtered through cotton wool and the peptide precipitated in a 50 mL falcon tube in Tert-butyl methyl ether at 0 ˚C. The suspension was centrifuged to a pellet for 20 minutes at 1500 rpm and the filtrate was removed by decantation. The pellet was placed under high vacuum to remove residual traces of solvent. Alternatively, the pellet was dissolved in water and lyophilized to a powder. Diastereoisomeric mixture was then purified on a Waters Mass-triggered preparative HPLC system paired with a x-SELECT CSH Prep C18 5µm column using a 10-25% gradient of acetonitrile with 0.1% Formic Acid. Pure diastereoisomers were characterized on mass spectra (Waters UPLC system) followed by lyophilization of pure fractions and subsequently dissolved in distilled water prior to use.

HRMS m/z calculated for $C_{70}H_{115}N_{19}O_{14}S_2$: 755.9229 $(M+2H^+)/2$, m/z observed: 755.9256 $(M+2H^+)/2$

Standard procedure for the synthesis of the octapeptides for N-terminal attachment.

Firstly, Fmoc-L-Ala-OH (3 eq.) was attached on Rink amide resin using [O-(7-azabenzotriazol-1-yl)-1,1,3,3-tetramethyluronium hexafluorophosphate] (HATU) and N,N-diisopropylethylamine (3 eq.) in DMF. Loading was controlled by UV measurement (λ=301nm and 290nm) of dibenzofulvene using spectrophotometer and Cuvette: Hellma 104-QS, Suprasil Quartz Z600288 10mm, 200-2500 nm (Mean Loading= 0.45 mmol/g). Synthesis was pursued with standard Fmoc/t-Bu protected amino acids (3 eq.) in the presence of [O-(7-azabenzotriazol-1-yl)-1,1,3,3-tetramethyluronium hexafluorophosphate] HATU (3 equiv.), N,N-diisopropylethylamine (9 eq.) in DMF (5 mL). After each coupling, Kaiser test was done to monitor completion. Deprotection was assessed using 50%Piperidine in DMF for 20 minutes.

Incorporation of Bromoacetic acid linker.

Symmetric 2-bromoacetic anhydride was prepared using bromoacetic acid (10 eq., 35.4 mg, 0.255 mmol) and N,N-Diisopropylcarbodiimide (5 eq., 19.7 µL, 0.127 mmol) in DCM. The mixture was stirred at r.t for 15 minutes. The solution of freshly prepared symetric 2-bromoacetic anhydride was added onto the N-terminus deprotected resin and stirred for 30 minutes to provide the bromo-intermediate. Completion of the reaction was monitored by UPLC MS.

Attachment of compound 11 of the octapeptides in N-terminus position (Compound **18)**.

Compound **11** was coupled to the peptides using standard type 2 nucleophilic substitution in the presence of DIPEA in DMF. Compound **11** (1.5 eq. 16.2 mg, 0.038 mmoles) and DIPEA (6 eq., 26.4 µL, 0.152 mmoles) were added to the bromo intermediate and the mixture was stirred at r.t overnight to provide compound **18**.

Peptide was cleaved using 95% TFA, 2.5% TIPS, 2,5% H_2O for at least 2 hours.

The resin suspension was filtered through cotton wool and the peptide precipitated in a 50 mL Falcon tube in tert-butyl methyl ether at 0 ˚C. The suspension was centrifuged to a pellet for 20 minutes at 1500 rpm and the filtrate removed by decanting. The pellet was placed under high vacuum to remove residual traces of solvent. Alternatively, the pellet was dissolved in water and lyophilized to a powder. Peptides were then purified on a Waters Mass-triggered preparative HPLC system paired with a x-SELECT CSH Prep C18 5µm column using a 10-25% gradient of acetonitrile with 0.1% Formic Acid. The pure peptides were characterized by UPLC followed by lyophilization of pure fractions and subsequently dissolved in distilled water prior to use

HRMS m/z calculated for $C_{61}H_{99}N_{17}O_{13}S_2$: 671.8598 $(M+2H^+)/2$, m/z observed: 671.8612 $(M+2H^+)/2$

Bioassays

Cell culture.

HEK293 cells stably expressing CXCR4 tagged with Hemagglutinin (refered as HA-CXCR4) were cultured in Dulbecco's Modified Eagle Medium supplemented with 10% FBS and 100 IU/mL penicillin, and 100µg/mL streptomycin in a 5% CO2 atmosphere. Cells stably expressing hCXCR4 were grown using puromycin (3 µg/mL) as a selection agent. At a confluence of 95% in 10 cm diameter Petri dishes, cells were readily used for binding assays.

Binding affinity.

Competitive binding assays, as previously described using ^{125}I-CXCL12 were assessed to obtain IC50 values. HEK293 cells stably expressing hCXCR4 were washed with PBS and subjected to a freeze–thaw cycle. Broken cells were then gently scraped in resuspension buffer (50 mM Hepes,

pH 7.4, 1 mM $CaCl_2$, and 5 mM $MgCl_2$), centrifuged at 3500 RPM for 15 min at 4 °C, and resuspended in binding buffer (50 mM Hepes, pH 7.4, 1 mM $CaCl_2$, 5 mM $MgCl_2$, 140 mM NaCl, and 0.1% BSA). For competition binding assays, 1 µg of receptor protein were incubated for 1 h at room temperature in binding buffer with 0.03 nM [^{125}I]-CXCL12 as a tracer and increasing concentrations of ligand in a final volume of 500µL. Bound radioactivity was separated from free ligand by filtration, and a gamma counter quantified receptor-bound radioactivity. Radioligand binding assays were collected in triplicate and are presented as means ± SEMs.

***In vitro* chemotaxis.**

Transwell cell migration assays were performed on acute lymphoblastic B-cell leukemia (also known as REH cells). Cells were first washed using RPMI medium, and 100000 cells, suspended in 25µL medium containing RPMI medium with 0.2% BSA. 100000 cells were seeded per well on a 96-well migration assay plates (5 µm pore size polycarbonate membrane; Neuroprobe ChemoTx system). Dilutions of the various peptides (in RPMI medium + 0.2% BSA) were added to the bottom chamber in a final volume of 29 µL. Neuroprobe ChemoTx system were incubated for 3h at 37 °C in a 5% CO_2 atmosphere. Subsequently to incubation, the migrated cells located in the lower chamber were counted using a BIORAD T10 automated cell counter. Data were compiled and represented as the percentage of the 100000 cells initially seeded onto the plate that have migrated to the bottom chamber of the plate. Maxima of migration values were calculated from 3 independent experiments, each performed in triplicate.

BRET experiments

G protein activation.

To monitor direct G protein activation, we used the previously described protocol for G-protein activation[55]. For our experiment, we used the biosensors $G\alpha_i$-91-RlucII, $G\beta_1$, and GFP^{10}-$G\gamma_1$. Biosensors were co-transfected with human HA-CXCR4 or HA-CXCR4 N119S in HEK293 cells using polyethylenimine in 100-mm dishes seeded with 3×10^6 cells. 24h post-transfection, 100000 cells per well were distributed in a 96-well microplate.

48 hours after transfection, cells were washed with HBSS complemented with 0.1% BSA and then, incubated with various concentrations of CXCL12 or chimeras (10^{-12} to 10^{-5} M) for 7 minutes and then completed with coelenterazine-400A to a final concentration of 5µM. Plate read out were obtained using a M1000 plate reader where the BRET2 filters were set to monitor the emission ratio (ratio of GFP^{10} emission at 515 nm over emission of RlucII at 400 nm)

EC_{50} values were calculated from three independent experiments, each performed in triplicate.

pA2 experiments monitored by BRET.

$G\alpha_i$-91-RlucII, $G\beta_1$, and GFP^{10}-$G\gamma_1$ were cotransfected with human HA-CXCR4 in HEK293 cells using polyethylenimine in 100-mm dishes seeded with 3×10^6 cells. 24h post-transfection, 100,000 cells per well were distributed in a 96-well microplate. 48 hours after transfection, cells were washed with HBSS complemented with 0.1% BSA and then, incubated for 7 minutes with various concentrations of CXCL12 (10^{-12} to 10^{-5} M) and fixed concentrations of antagonists between 10 and 100 nM.

All wells were completed with coelenterazine-400A to a final concentration of 5µM and plates were immediately read out on a M1000 plate reader where the BRET2 filters.

pA2 values were calculated from 3 independent experiments each performed in triplicate using Schild method and the equation log (dose ratio – 1) = log([B]) – log(kB). Schild curves were plotted using GraphPad Prism 6 and pA2 values were obtained when log (dose ratio – 1) = 0

β-arrestin2 recruitment assay.

BRET-β-arrestin2 recruitment experiments, were done like described previously with G protein activation. Briefly, HEK293 cells were co-transfected with CXCR4-RLuc3 or CXCR4-RLuc3 N119S and GFP[10]-β-arrestin-2. 48 hours after transfection, cells were incubated with various concentrations of CXCL12 or chimeras (10^{-12} to 10^{-5} M) for 20 minutes and then completed with coelenterazine-400A. Plate read out were obtained using a M1000 plate reader where the BRET2 filters were set to monitor the 515 nm/400 nm emission ratio.

EC50 values were calculated from three independent experiments, each performed in triplicate.

Molecular dynamic simulations

The isomers of compound **11** and **12** were manually generated from the crystal structure of IT1t using the "Build" function in PyMOL (The PyMOL Molecular Graphics System, Version 1.7 Schrödinger, LLC.) and parametrized for the Gromos 54A7 forcefield using the Automated Topology Builder.[56] The ligands were manually docked in the CXCR4 receptor by superposition over the IT1t molecule in the crystal structure of CXCR4 in complex with IT1t[33] (PDB code 3oe6). The receptor-ligand complexes were solvated using the SPC water model.[57] Sodium and chlorine atoms were added at random positions, replacing water molecules, to keep the net charge of the system at 0 and provide an approximate concentration of 150 mM NaCl. The GROMACS

software[58-61] was used to run the MD simulations with the Gromos 54a7 forcefield. Simulations were performed for a total of 2 nanoseconds (with 2 femtoseconds time steps) under NPT conditions, using the V-rescale thermostat and Berendsen barostat.[62] The systems were gradually heated from 0 K to 310 K during the first 500 picoseconds. Position restraints were applied to the backbone atoms of the receptor during the MD simulations.

ACKNOWLEDGEMENTS

Financial support from the Canadian Institutes of Health Research, the Natural Sciences & Engineering Research Council of Canada and the Canadian Foundation for Innovation is acknowledged. The Conseil Régional de la Martinique (France) is gratefully acknowledged for a scholarship to CM. Institut de Pharmacologie de Sherbrooke and Sherbrooke Neuroscience Centre are also acknowledged for a fellowship to E.B.O. Prof. J.-B. Denault and Dr. R. Gagnon are gratefully acknowledged for providing equipment for biological assays and HRMS, respectively. Dr. A. Le Roux and Dr. P.-L. Boudreault are acknowledged for helpful discussions. Finally, we would like to thank the CQDM team (M. Bouvier *et al*.) for sharing the BRET biosensors.

NOTES AND REFERENCES

1 A. E. I. Proudfoot, *Nat. Rev. Immunol.*, 2002, **2**, 106–115.

2 M. Thelen and S. Thelen, *J. Neuroimmunol.*, 2008, **198**, 9–13.

3 I. F. Charo and R. M. Ransohoff, *N. Engl. J. Med.*, 2006, **354**, 610–621.

4 C. Murdoch and A. Finn, *Blood*, 2000, **95**, 3032–3043.

5 C. D. Buckley, N. Amft, P. F. Bradfield, D. Pilling, E. Ross, F. Arenzana-Seisdedos, A. Amara, S. J. Curnow, J. M. Lord, D. Scheel-Toellner and M. Salmon, *J. Immunol.*, 2000, **165**, 3423–3429.

6 E. Vicenzi, P. Liò and G. Poli, *Theranostics*, **3**, 18–25.

7 E. A. Berger, P. M. Murphy and J. M. Farber, *Annu. Rev. Immunol.*, 1999, **17**, 657–700.

8 A. Zlotnik, A. M. Burkhardt and B. Homey, *Nat. Rev. Immunol.*, 2011, **11**, 597–606.

9 Q. Liu, H. Chen, T. Ojode, X. Gao, S. Anaya-O'Brien, N. A. Turner, J. Ulrick, R. DeCastro, C. Kelly, A. R. Cardones, S. H. Gold, E. I. Hwang, D. S. Wechsler, H. L. Malech, P. M. Murphy and D. H. McDermott, *Blood*, 2012, **120**, 181–189.

10 G. A. Diaz, *Blood*, 2011, **118**, 4764–4765.

11 T. J. Schall and A. E. I. Proudfoot, *Nat. Rev. Immunol.*, 2011, **11**, 355–363.

12 B. A. Teicher and S. P. Fricker, *Clin. Cancer Res.*, 2010, **16**, 2927–2931.

13 J. Quoyer, J. M. Janz, J. Luo, Y. Ren, S. Armando, V. Lukashova, J. L. Benovic, K. E. Carlson, S. W. Hunt and M. Bouvier, *Proc. Natl. Acad. Sci. U.S.A.*, 2013, **110**, E5088–97.

14 S. M. Rankin, *Immunol. Lett.*, 2012, **145**, 47–54.

15 D. J. Scholten, M. Canals, D. Maussang, L. Roumen, M. J. Smit, M. Wijtmans, C. de Graaf, H. F. Vischer and R. Leurs, *Br. J. Pharmacol.*, 2012, **165**, 1617–1643.

16 S. Gelmini, M. Mangoni, M. Serio, P. Romagnani and E. Lazzeri, *J. Endocrinol. Invest.*, 2008, **31**, 809–819.

17 M. Kucia, K. Jankowski, R. Reca, M. Wysoczynski, L. Bandura, D. J. Allendorf, J. Zhang, J. Ratajczak and M. Z. Ratajczak, *J. Mol. Histol.*, 2004, **35**, 233–245.

18 S. Chatterjee, B. Behnam Azad and S. Nimmagadda, *Adv. Cancer Res.*, 2014, **124**, 31–82.

19 P. Weitzenfeld and A. Ben-Baruch, *Cancer Lett. (N. Y., NY, U. S.)*, 2013, **352**, 36–53.

20 L. Portella, R. Vitale, S. De Luca, C. D'Alterio, C. Ieranò, M. Napolitano, A. Riccio, M. N. Polimeno, L. Monfregola, A. Barbieri, A. Luciano, A. Ciarmiello, C. Arra, G. Castello, P. Amodeo and S. Scala, *PLOS One*, 2013, **8**, e74548.

21 C. Peitzsch, I. Kurth, L. Kunz-Schughart, M. Baumann and A. Dubrovska, *Radiother. Oncol.*, 2013, **108**, 378–387.

22 M. Lefrançois, M.-R. Lefebvre, G. Saint-Onge, P. E. Boulais, S. Lamothe, R. Leduc, P. Lavigne, N. Heveker and E. Escher, *ACS Med. Chem. Lett.*, 2011, **2**, 597–602.

23 C. E. Mona, É. Besserer-Offroy, J. Cabana, M. Lefrançois, P. E. Boulais, M.-R. Lefebvre, R. Leduc, P. Lavigne, N. Heveker, E. Marsault and E. Escher, *J. Med. Chem.*, 2016, **59**, 7512–7524.

24 C. Herrera, C. Morimoto, J. Blanco, J. Mallol, F. Arenzana, C. Lluis and R. Franco, *J. Biol. Chem.*, 2001, **276**, 19532–19539.

25 N. Heveker, M. Montes, L. Germeroth, A. Amara, A. Trautmann, M. Alizon and J. Schneider-Mergener, *Curr. Biol.*, 1998, **8**, 369–376.

26 P. Loetscher, J. H. Gong, B. Dewald, M. Baggiolini and I. Clark-Lewis, *J. Biol. Chem.*, 1998, **273**, 22279–22283.

27 H. Lortat-Jacob, *Curr. Opin. Struct. Biol.*, 2009, **19**, 543–548.

28 J. W. Murphy, Y. Cho, A. Sachpatzidis, C. Fan, M. E. Hodsdon and E. Lolis, *J. Biol. Chem.*, 2007, **282**, 10018–10027.

29 Z. Luo, N. Zhou, J. Luo, J. W. Hall and Z. Huang, *Biochem. Biophys. Res. Commun.*, 1999, **263**, 691–695.

30 J. Luo, Z. Luo, N. Zhou, J. W. Hall and Z. Huang, *Biochem. Biophys. Res. Commun.*, 1999, **264**, 42–47.

31 Y. Kofuku, C. Yoshiura, T. Ueda, H. Terasawa, T. Hirai, S. Tominaga, M. Hirose, Y. Maeda, H. Takahashi, Y. Terashima, K. Matsushima and I. Shimada, *J. Biol. Chem.*, 2009, **284**, 35240–35250.

32 G. Thoma, M. B. Streiff, J. Kovarik, F. Glickman, T. Wagner, C. Beerli and H.-G. Zerwes, *J. Med. Chem.*, 2008, **51**, 7915–7920.

33 B. Wu, E. Y. T. Chien, C. D. Mol, G. Fenalti, W. Liu, V. Katritch, R. Abagyan, A. Brooun, P. Wells, F. C. Bi, D. J. Hamel, P. Kuhn, T. M. Handel, V. Cherezov and R. C. Stevens, *Science*, 2010, **330**, 1066–1071.

34 Y.-H. Joo and J. M. Shreeve, *Chem. Commun.*, 2010, **46**, 142–144.

35 Y.-H. Joo and J. M. Shreeve, *Inorg. Chem.*, 2009, **48**, 8431–8438.

36 T. Tsuji, H. Momona and T. Ueda, *Chem. Pharm. Bull.*, 1967, **15**, 936–943.

37 J. A. Ballesteros and H. Weinstein, *Methods Neurosci.*, 1995, **25**, 366–428.

38 H. Levine and W.-J. Rappel, *Phys. Today*, 2013, **66**, 1–14.

39 W. B. Zhang, J. M. Navenot, B. Haribabu, H. Tamamura, K. Hiramatu, A. Omagari, G. Pei, J. P. Manfredi, N. Fujii, J. R. Broach and S. C. Peiper, *J. Biol. Chem.*, 2002, **277**, 24515–24521.

40 H. Tamamura, Y. Xu, T. Hattori, X. Zhang, R. Arakaki, K. Kanbara, A. Omagari, A. Otaka, T. Ibuka, N. Yamamoto, H. Nakashima and N. Fujii, *Biochem. Biophys. Res. Commun.*, 1998, **253**, 877–882.

41 T. Kenakin, *Mol. Pharmacol.*, 2004, **65**, 2–11.

42 L. A. Thompson and J. A. Ellman, *Tetrahedron Lett.*, 1994, **35**, 9333–9336.

43 E. K. Kick and J. A. Ellman, *J. Med. Chem.*, 1995, **38**, 1427–1430.

44 L. Qin, I. Kufareva, L. G. Holden, C. Wang, Y. Zheng, C. Zhao, G. Fenalti, H. Wu, G. W. Han, V. Cherezov, R. Abagyan, R. C. Stevens and T. M. Handel, *Science*, 2015, **347**, 1117–1122.

45 M. P. Wescott, I. Kufareva, C. Paes, J. R. Goodman, Y. Thaker, B. A. Puffer, E. Berdougo, J. B. Rucker, T. M. Handel and B. J. Doranz, *Proc. Natl. Acad. Sci. U.S.A.*, 2016, **113**, 9928–9933.

46 M. P. Crump, J. H. Gong, P. Loetscher, K. Rajarathnam, A. Amara, F. Arenzana-Seisdedos, J. L. Virelizier, M. Baggiolini, B. D. Sykes and I. Clark-Lewis, *EMBO J.*, 1997, **16**, 6996–7007.

47 G. Besenyei, S. Németh and L. I. Simándi, *Tetrahedron Lett.*, 1993, **34**, 6105–6106.

48 P. Dauban and R. H. Dodd, *Tetrahedron Lett.*, 1998, **39**, 5739–5742.

49 B. G. Burgaud, D. C. Horwell, A. Padova and M. C. Pritchard, *Tetrahedron*, 1996, **52**, 13035–13050.

50 G. Thoma, M. B. Streiff, J. Kovarik, F. Glickman, T. Wagner, C. Beerli and H.-G. Zerwes, *J. Med. Chem.*, 2008, **51**, 7915–7920.

51 K. Feichtinger, H. L. Sings, T. J. Baker, K. Matthews and M. Goodman, *J. Org. Chem.*, 1998, **63**, 8432–8439.

52 A. Mahindra, K. K. Sharma and R. Jain, *Tetrahedron Lett.*, 2012, **53**, 6931–6935.

53 C. Ghosh, G. B. Manjunath, P. Akkapeddi, V. Yarlagadda, J. Hoque, D. S. S. M. Uppu, M. M. Konai and J. Haldar, *J. Med. Chem.*, 2014, **57**, 1428–1436.

54 D. A. Nugiel, L. A. Cornelius and J. W. Corbett, *J. Org. Chem.*, 1997, **62**, 201–203.

55 M. Demeule, N. Beaudet, A. Régina, É. Besserer-Offroy, A. Murza, P. Tétreault, K. Belleville, C. Ché, A. Larocque, C. Thiot, R. Béliveau, J.-M. Longpré, E. Marsault, R. Leduc, J. E. Lachowicz, S. L. Gonias, J.-P. Castaigne and P. Sarret, *J. Clin. Invest.*, 2014, **124**, 1199–1213.

56 A. K. Malde, L. Zuo, M. Breeze, M. Stroet, D. Poger, P. C. Nair, C. Oostenbrink and A. E. Mark, *J. Chem. Theory Comput.*, 2011, **7**, 4026–4037.

57 C. D. Berweger and W. F. van Gunsteren, *Chem. Phys. Lett.*, 1995, **232**, 429–436.

58 H. Berendsen and D. van der Spoel, *Comput. Phys. Commun.*, 1995, **91**, 43–56.

59 D. van der Spoel, E. Lindahl, B. Hess, G. Groenhof, A. E. Mark and H. J. C. Berendsen, *J. Comput. Chem.*, 2005, **26**, 1701–1718.

60 B. Hess, C. Kutzner, D. van der Spoel and E. Lindahl, *J. Chem. Theory Comput.*, 2008, **4**, 435–447.

61 D. van der Spoel and B. Hess, *Wiley Interdiscip. Rev.: Comput. Mol. Sci.*, 2011, **1**, 710–715.

62 G. Bussi, T. Zykova-Timan and M. Parrinello, *J. Chem. Phys.*, 2009, **130**, 074101.

SCHEMES

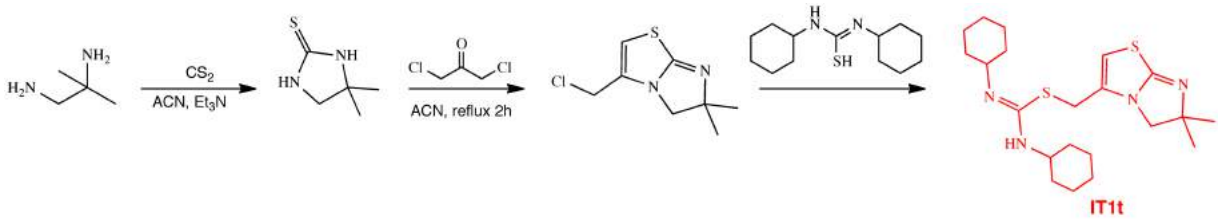

Scheme 1. IT1t synthetic strategy.

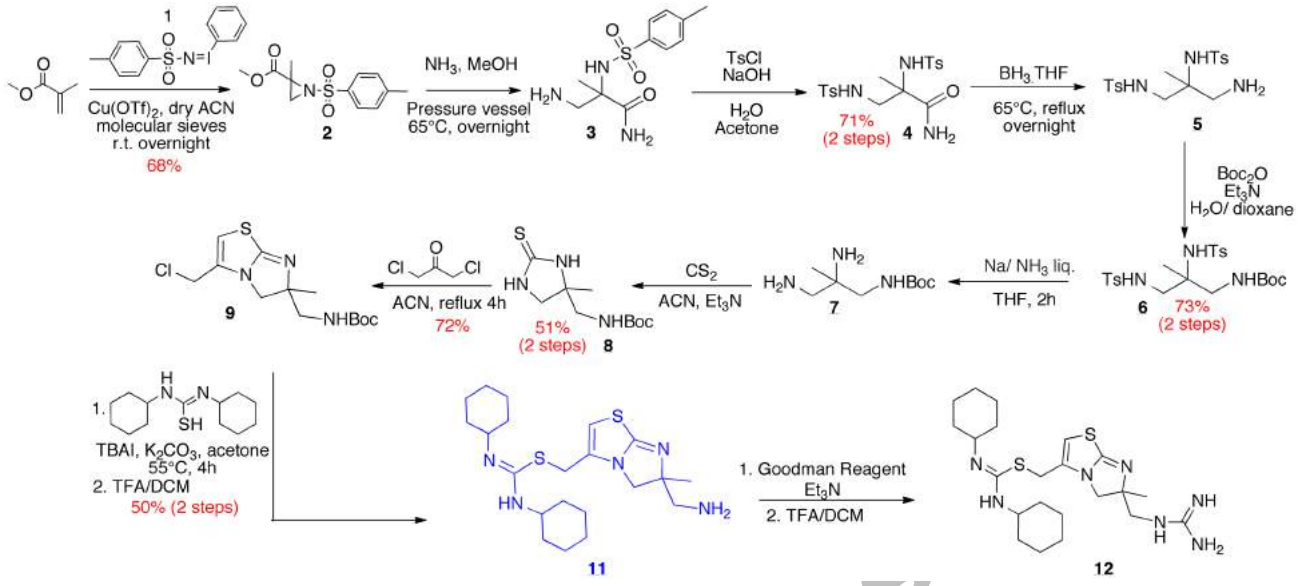

Scheme 2. IT1t-like molecules synthetic strategy.

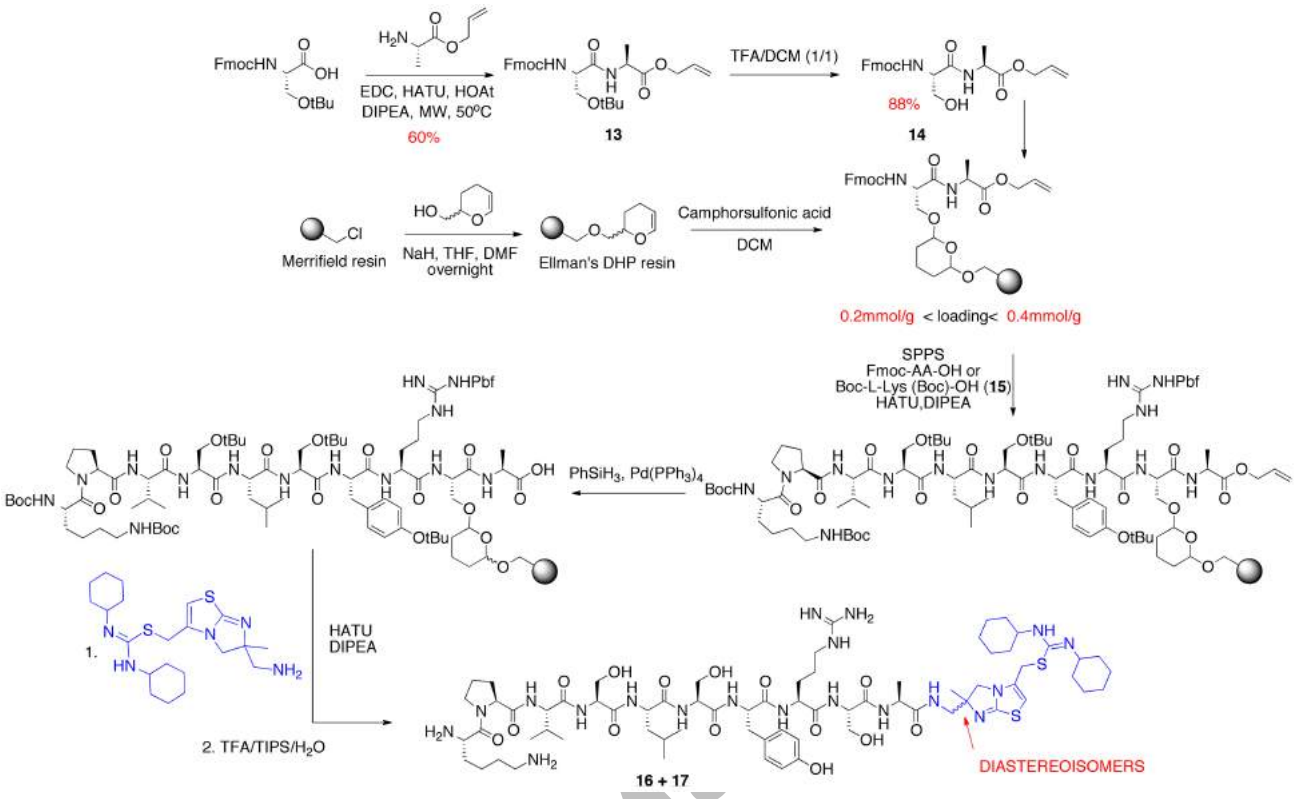

Scheme 3. C-terminus attachment.

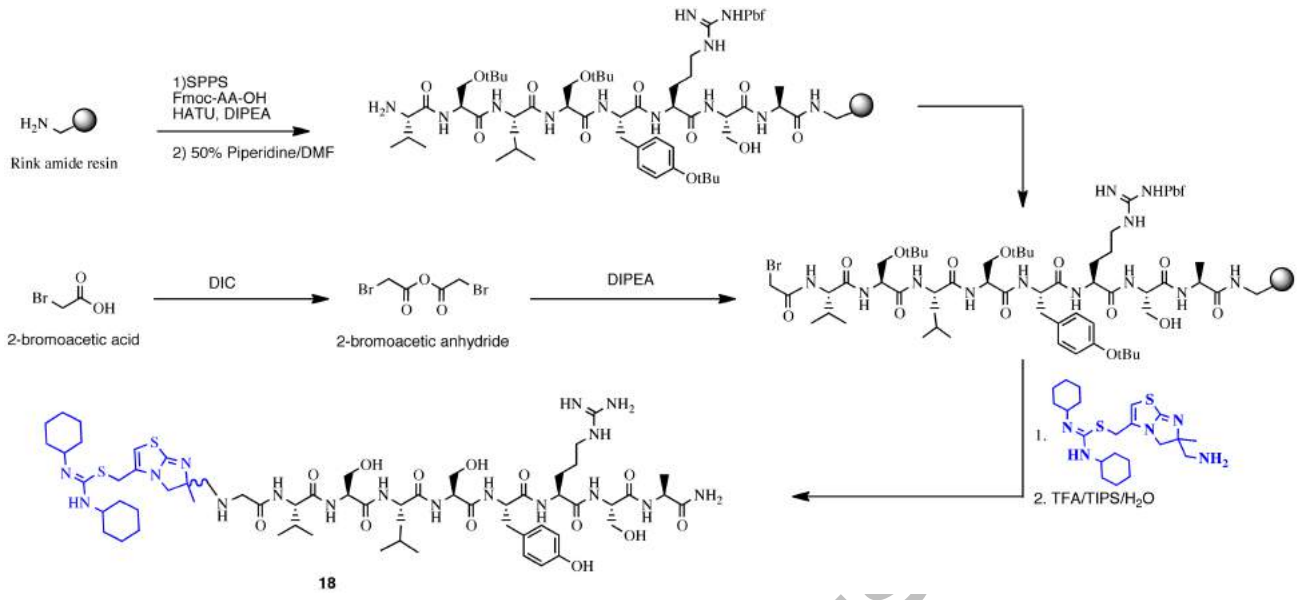

Scheme 4. N-terminus attachment.

FIGURES

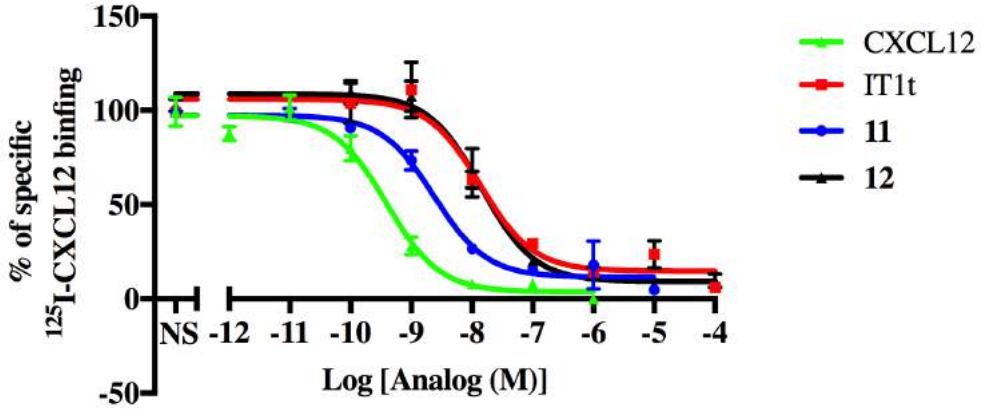

Figure 1. Competition binding assay with ^{125}I-CXCL12 of CXCL12, IT1t, compounds **11** and **12** on HEK293 cells stably expressing the human HA-tagged CXCR4 receptor.

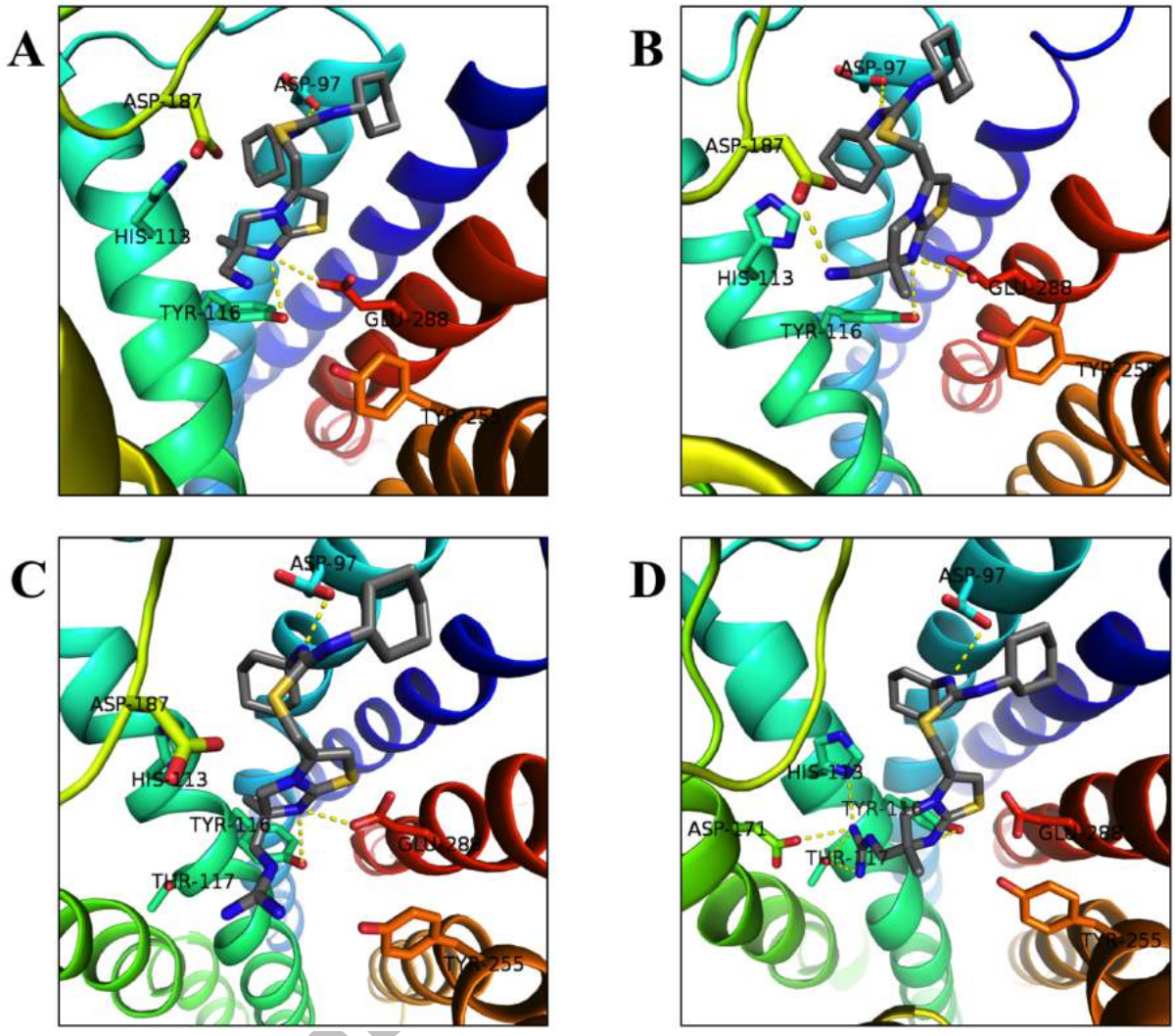

Figure 2. Snapshots of MD simulations showing interactions of each enantiomer of analogs **11** (**A-B**) and **12** (**C-D**).

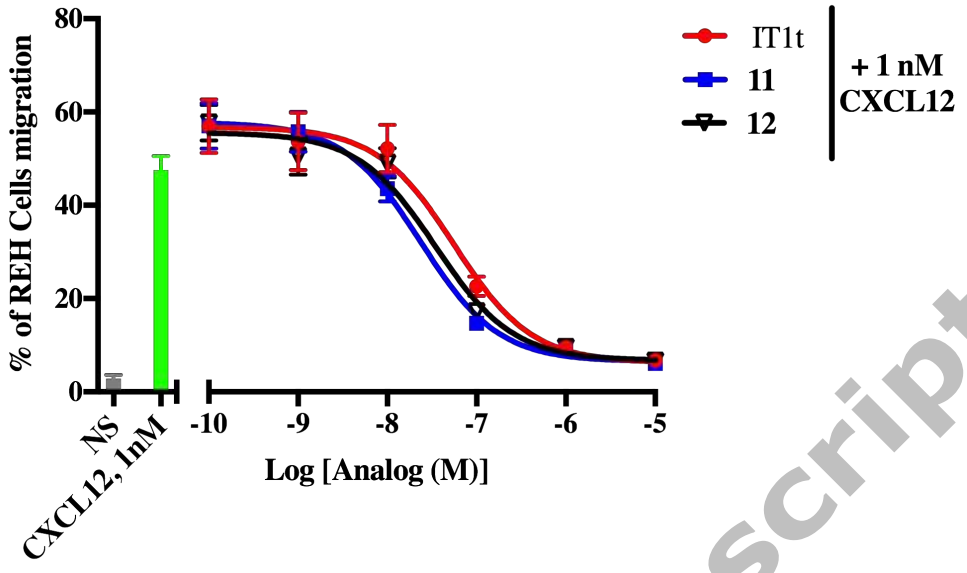

Figure 3. CXCL12-induced chemotaxis assay. Inhibition of CXCL12-induced migration by IT1t, compound **11** or compound **12** was assessed with pre-B lymphocytes using Transwell migration assays.

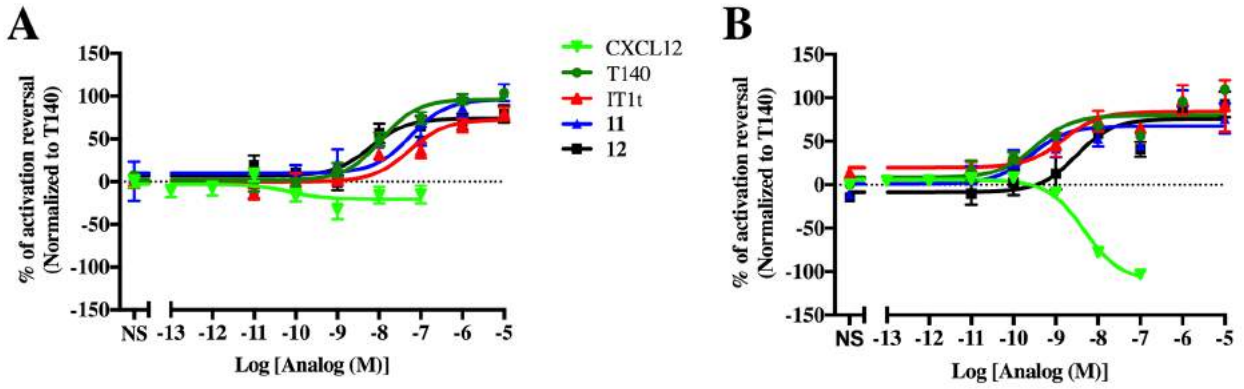

Figure 4. Effect of CXCl12, T140, IT1t, compounds **11** and **12** on HEK293 cells expressing the constitutively active mutant of the human HA-tagged CXCR4 receptor (CXCR4-N119S). **A**. Concentration-response curves for the $G\alpha_i$ pathway and **B**. Concentration-response curves for β-arrestin-2 recruitment.

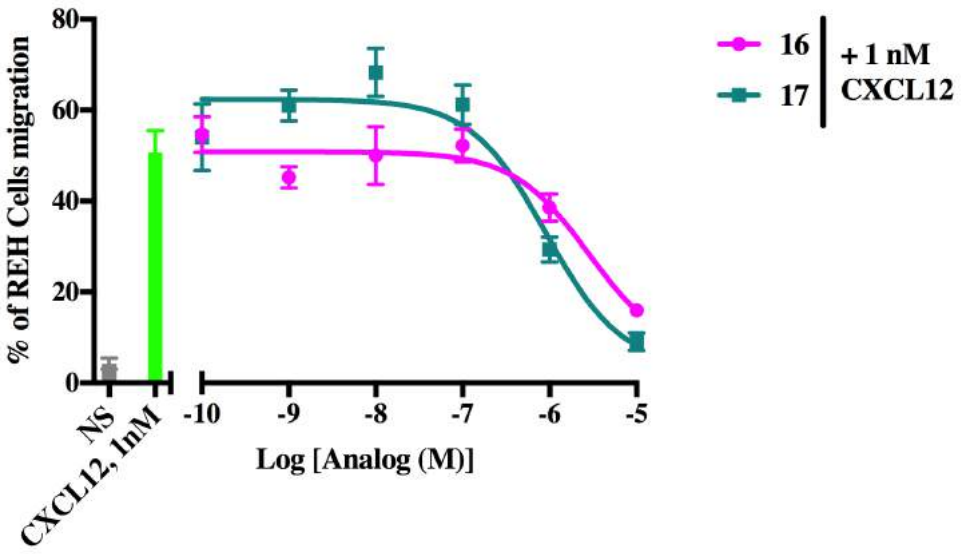

Figure 5. CXCL12-induced chemotaxis assay. Inhibition of CXCL12-induced migration by compounds **16** and **17** was assessed with pre-B lymphocytes using Transwell migration assays.